PZT

王 兴[1], 邹赫麟[2]
(1. , 030032; 2. , , 116024)

: , Pt/Ti (PZT) ,
PZT X (XRD)
(SEM) , , Pt , , PZT
Pt/Ti 200 30 min , PZT (100) ,
Pt/Ti PZT (111) , Pt/Ti
200 30 min , PZT , ,
10^8 , 11%
: Pt/Ti ; ; ; ; ;
: TM223 : A : 1001-1625(2023)02-0743-08

Influences of In-Situ Annealing and Deposition Temperature of Bottom Electrodes on Properties of PZT Films

WANG Xing[1], *ZOU Helin*[2]
(1. Department of Electromechanical and Vehicle Engineering, Taiyuan University, Taiyuan 030032, China;
2. Key Laboratory for Micro/Nano Technology and System of Liaoning Province, Dalian University of Technology, Dalian 116024, China)

Abstract: Lead zirconium titanate (PZT) films were deposited on Pt/Ti bottom electrode by magnetron sputtering process. The influences of in-situ annealing temperature and electrode deposition temperature on crystal orientation, microstructure, dielectric, ferroelectric, and fatigue characteristics of sputtered PZT films were studied. The results of X-ray diffraction (XRD) and scanning electron microscope (SEM) analysis show that as the electrode deposition temperature increases, the Pt crystal grain size increases, and as the annealing temperature increases, the PZT film compactness becomes worse. The Pt/Ti bottom electrode prepared at room temperature after in-situ annealed in 200 for 30 min can easily promote the (100) orientation of the PZT film, while the Pt/Ti bottom electrode prepared or annealed at high temperature is more conducive to the (111) orientation. The best dielectric property is obtained in the PZT film according to electrical tests, in which the Pt/Ti bottom electrode is prepared at room temperature and in-situ annealed in 200 for 30 min. And the PZT film exhibits high residual polarization strength and minimum coercive field strength. After 10^8 times polarization inversions, the initial polarization of the film drop is only 11%.
Key words: Pt/Ti bottom electrode; piezoelectric film; in-situ annealing; preferred orientation; dielectric property; fatigue characteristic

0 引 言

, ,
(micro-electro-mechanical system, MEMS) [1-3] ,

: 2022-08-17; : 2022-11-03
: (51775088); (202203021212017)
: (1987—), , , E-mail: wangxing010@126.com

, (lead zirconium titanate, PZT) ,
[4-5]
,
[6-8] , PZT :
,
[9-10] [11]
, PZT , , Fujii
[12] Si MgO , (001) PZT ,
100 150 pm/V, Miyazaki [13] PZT
, $SrRuO_3$ (SRO) / Si Pt/Ti PZT , , SRO
PZT (110) , Pt/Ti (100)
, PZT , ,
[14-15] , , Pt/Ti
, PZT (a[PZT] = 0.407 7 nm, a[Pt] = 0.392 2 nm),
[16] Pt/Ti , ,
Ti/TiO_2 Jeong [17] Pt/TiO_x , PZT
Vilquin[18] , (400 ~ 600),
Pt/TiO_2 , , $Pb(Zr_{0.70}, Ti_{0.30})O_3$ (100)
, Pt/Ti PZT
, Pt/Ti PZT

, (25 250 300 400 450 500) Pt/Ti
, Pt ; $Pb(Zr_{0.52}Ti_{0.48})O_3$,
Pt/Ti PZT

1 实 验

1.1 Pt/Ti PZT

1.1.1 Pt/Ti

Pt/Ti SiO_2/Si ,
99.99% Pt Ti , 25 250 300 400 450 500
3.0×10^{-5} Pa Ar (15 mL/min), 0.5 Pa, 1
Pt/Ti
(25) Pt/Ti , 100 200 300 400 500 ,
30 min,

1 Pt/Ti

Table 1 Process parameters of preparing Pt/Ti bottom electrode by sputtering

Parameter settin	Parameter
Magnetron sputtering power/W	150
Target-substrate distance/mm	100
Base pressure/Pa	3.0×10^{-5}
Sputtering pressure/Pa	1
Substrate temperature/	25, 250, 300, 400, 450, 500
Sputtering gas	Pure argon (15 mL/min)

1.1.2 PZT

, $Pb(Zr_{0.52}Ti_{0.48})O_3$ PbO(99%) ZrO_2(99.5%) TiO_2(99.5%)

( ), QM-3SP2 3 h,
(m( ) m( ) m( ) = 2 1 0.5) , 800 2 h,
24 h , , ,
600 15 min , 2 h(1 200),
PZT
, Pt/Ti PZT Pt/Ti
5 min, , 3.0×10^{-5} Pa
, Ar/O_2 90/5 Ar O_2 , 1.5 Pa ,
2 h , 350 8 min, 600 30 min 2

2 PZT

Table 2 Sputtering parameters of PZT films

Target	$Pb(Zr_{0.52},Ti_{0.48})O_3$ ceramic disc
Target diameter/mm	60
Magnetron sputtering power/W	100
Base pressure/Pa	3.0×10^{-5}
Sputtering pressure/Pa	1.5
Sputtering temperature/	Room temperature
Sputtering gas	Ar/O_2 (90/5)
Annealing parameter	Preheated at 350 for 8 min, annealed at 600 for 30 min

1.2

Zeiss D8 Bruker X PZT Pt/Ti ,
20°~60°, 0.02°
Hitachi SU8200 (scanning electron microscopy, SEM) PZT

4294A PZT , 0.1~100 kHz,
1 V
HA-405 DG1022U DS1000U , Sawyer-Tower ,
[19-20] , 10 kHz M
P_M P_r P_{hormal}, (1)

$$P_{normal} = \frac{P_M}{P_r} \tag{1}$$

2 结果与讨论

2.1

2.1.1 PZT
Pt/Ti PZT
, XRD 1 ,
(P_v),
Pt/Ti 450 ,PZT
(100) , (111)
500 ,PZT
(111) ,
Ti Pt , PZT
, (111) [21]

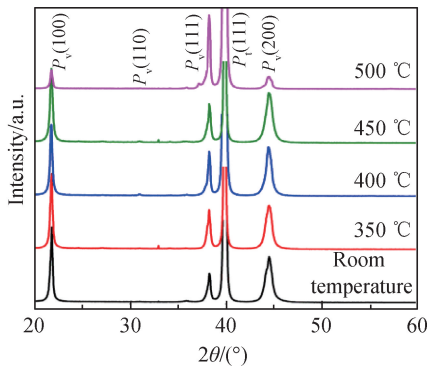

1 Pt/Ti PZT XRD
Fig.1 Effect of Pt/Ti bottom electrode deposition temperature on XRD pattern of PZT films

2.1.2 PZT

(200 300 400 500) Pt/Ti PZT , XRD

2(a) , , (100) (110) (111) (100)

α, 2(b) ,α , PZT

200 300 Pt/Ti , PZT (100)

, 58.1% 49.2% 400 ,PZT (111)

Pt 500 PZT 3 4

, (100) ,

, PZT (111) [21]

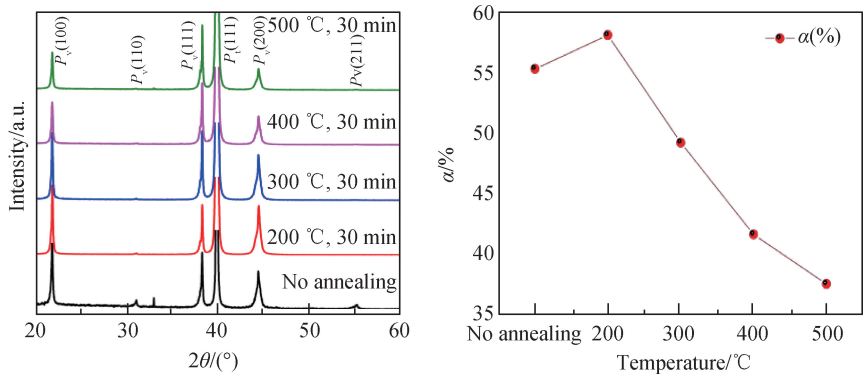

(a) XRD patterns (b) (100) orientation degree of films

2 PZT

Fig. 2 Influence of electrode in-situ annealing temperature on texture of PZT films

2.2

3 Pt/Ti PZT SEM , PZT

(3(a)) , , Pt/Ti 400 ,

PZT (3(b)) , 450 500 ,PZT

, (3(c) (d)) 3(e) 3(f)

30 min PZT Pt/Ti , 200

400 ,PZT 3(a) , 200 Pt/Ti PZT

Pt/Ti PZT , Pt/Ti ,

4 4(a) , , , 30 ~ 50 nm

Pt/Ti 400 (4(b)) , , ,

450 (4(c) (d)) , ,

, Pt/Ti ,

(30 min) , 5

(4(a)) , 200 (5(b)) Pt/Ti

300 400 (5(c) (d)) , , 500

(5(e)) , , 4 5

, PZT [22]

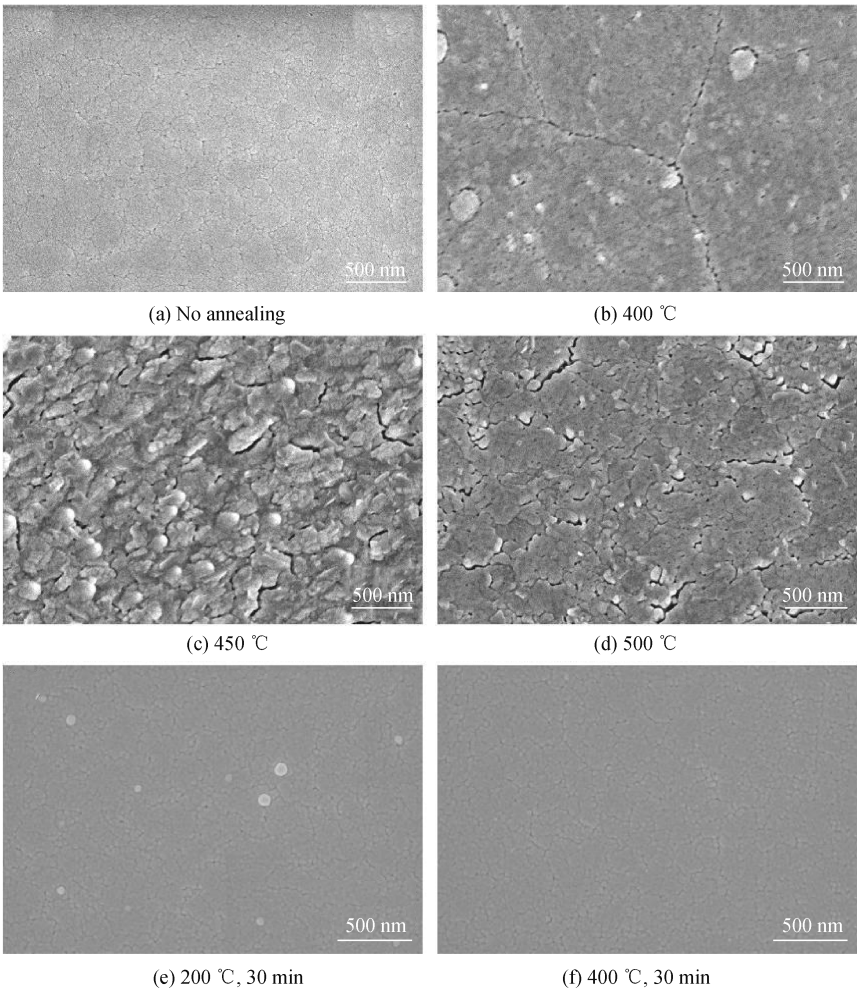

(a) No annealing (b) 400 ℃

(c) 450 ℃ (d) 500 ℃

(e) 200 ℃, 30 min (f) 400 ℃, 30 min

3 Pt/Ti PZT

Fig. 3 Effects of Pt/Ti bottom electrode preparation temperature and annealing temperature on surface morphology of PZT films

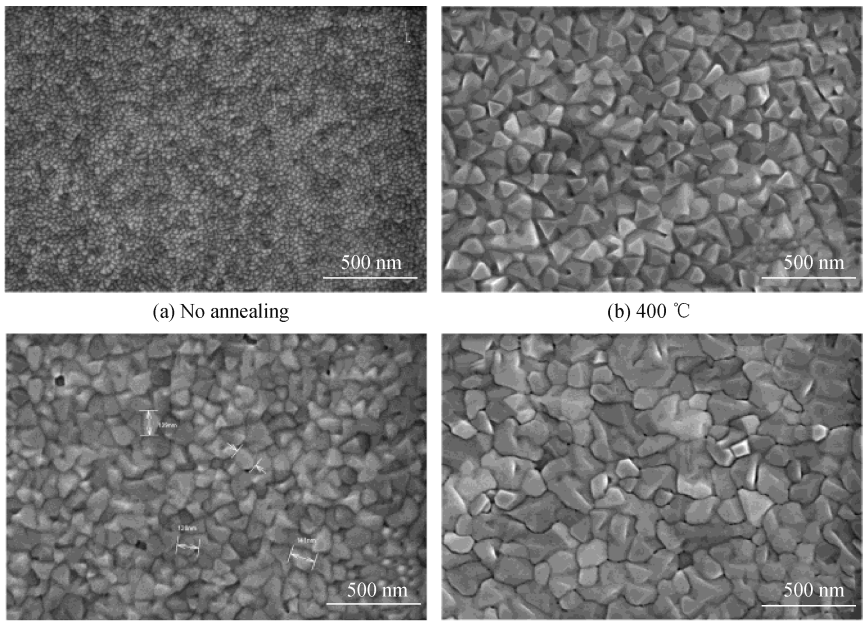

(a) No annealing (b) 400 ℃

(c) 450 ℃ (d) 500 ℃

4 Pt/Ti SEM

Fig. 4 SEM images of Pt/Ti bottom electrode at various preparation temperatures

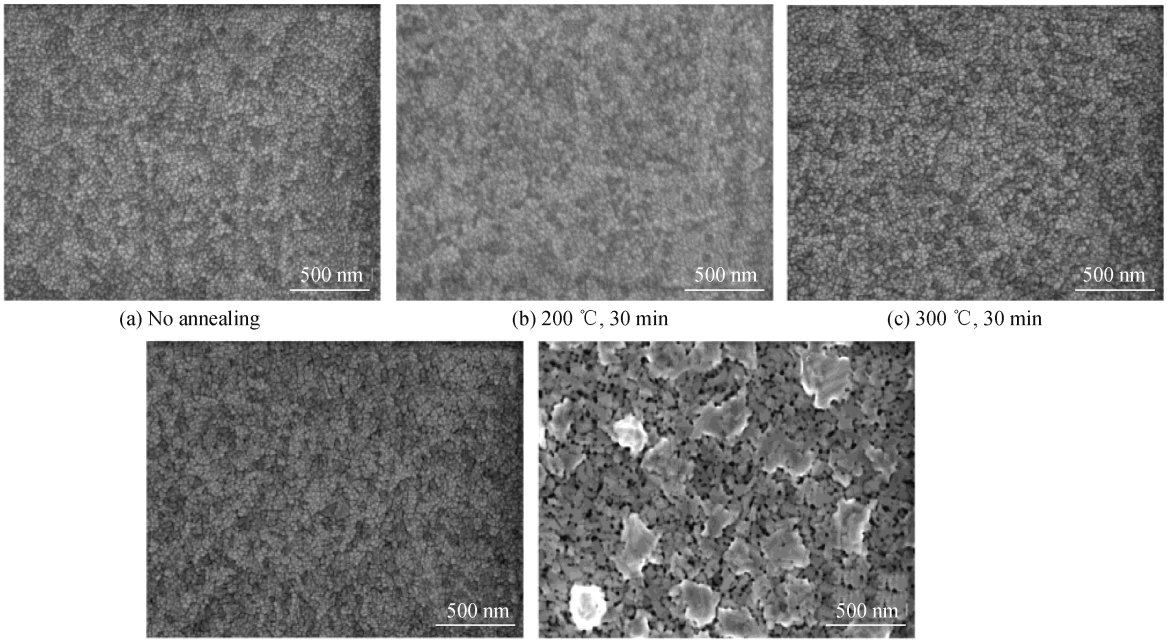

(a) No annealing (b) 200 ℃, 30 min (c) 300 ℃, 30 min

(d) 400 ℃, 30 min (e) 500 ℃, 30 min

5 Pt/Ti SEM

Fig. 5 SEM images of Pt/Ti bottom electrodes after in-situ annealing

2.3

2.3.1

PZT , ε_r tan δ (0.1 ~ 100 kHz) , 6 6(a) , , ε_r , , ε_r , [23-24] ε_r, tan δ , [25] Pt/Ti PZT , SEM , , ε_r tan δ , , [26] 400 ,500 PZT , (3), , ε_r 200 30 min Pt/Ti , PZT , 0.1 kHz ε_r 1 054, 500 Pt/Ti 10% 13% XRD SEM ,(100) , , ε_r , (100) [27]

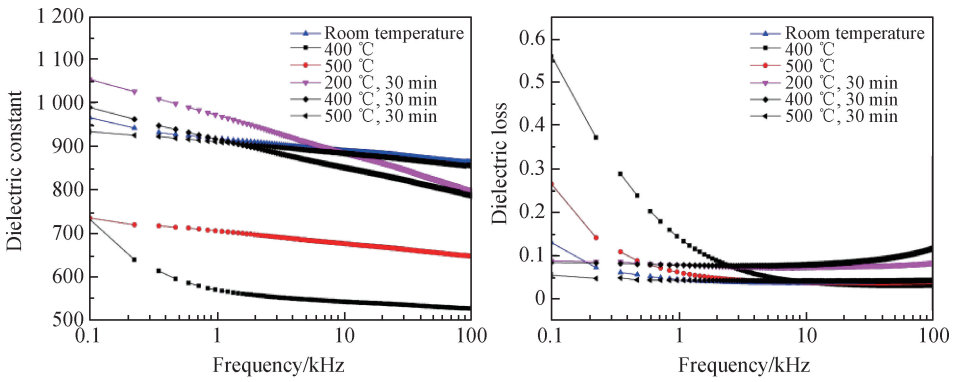

(a) ε_r as a function of frequency (b) tan δ as a function of frequency

6 PZT

Fig. 6 Dielectric properties of PZT films

2.3.2

Pt/Ti 200 400 30 min Pt PZT -
(P-E) 7(a) , ,
P-E , /
, [28] , PZT P_r
E_c , PZT P-E
400 30 min Pt/Ti ,200 Pt/Ti PZT
, E_c , ,
, , E_c 10 kHz 7(b)
10^7 , [29] 10^8 , 200 30 min
Pt/Ti , PZT , 11% ,
(5(b)) / [30] , ,

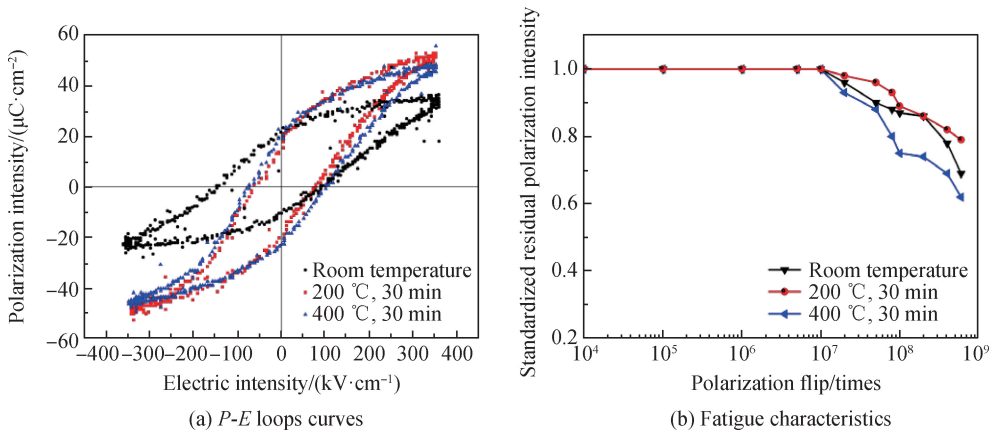

(a) P-E loops curves (b) Fatigue characteristics

7 PZT

Fig. 7 Ferroelectric properties and fatigue characteristics of PZT films

3 结 论

, Pt/Ti , Pt/Ti
, Pt/Ti PZT , (100) (111)
PZT , PZT MEMS
:

1) PZT ,Pt
, , 200 Pt/Ti ,

2) Pt/Ti 30 min (200) , PZT (100) ,
Pt PZT (111)

3) Pt/Ti , 200 30 min , PZT ,
0.1 kHz 1 054 , , 10^8
, 11%

[1] LI F, CABRAL M J, XU B, et al. Giant piezoelectricity of Sm-doped Pb($Mg_{1/3}Nb_{2/3}$)O_3-$PbTiO_3$ single crystals[J]. Science, 2019, 364(6437): 264-268.

[2] HAERTLING G H. Ferroelectric ceramics: history and technology[J]. Journal of the American Ceramic Society, 1999, 82(4): 797-818.

[3] YEO H G, XUE T C, ROUNDY S, et al. Strongly (001) oriented bimorph PZT film on metal foils grown by rf-sputtering for wrist-worn piezoelectric energy harvesters[J]. Advanced Functional Materials, 2018, 28(36): 1801327.

[4] BAEK S H, PARK J, KIM D M, et al. Giant piezoelectricity on Si for hyperactive MEMS[J]. Science, 2011, 334(6058): 958-961.

[5] GEORGE J P, SMET P F, BOTTERMAN J, et al. Lanthanide-assisted deposition of strongly electro-optic PZT thin films on silicon: toward integrated active nanophotonic devices[J]. ACS Applied Materials & Interfaces, 2015, 7(24): 13350-13359.

[6] HAN C S, PARK K S, CHOI H J, et al. Origin of in situ domain formation of heavily Nb-doped Pb(Zr, Ti)O_3 thin films sputtered on Ir/TiW/SiO_2/Si substrates for mobile sensor applications[J]. ACS Applied Materials & Interfaces, 2017, 9(22): 18904-18910.

[7] NICOLAS S, ALLAIN M, BRIDOUX C, et al. Fabrication and characterization of a new varifocal liquid lens with embedded PZT actuators for high optical performances[C]//2015 28th IEEE International Conference on Micro Electro Mechanical Systems (MEMS). January 18-22, 2015, Estoril, Portugal. IEEE, 2015: 65-68.

[8] , , , . [J]. , 2019, 38(11): 3403-3408.
XIE D D, ZHOU J, WU Z, et al. Inhibition of leakage current in lead zirconate titanate thin films by barium magnesium niobate buffer layer[J]. Bulletin of the Chinese Ceramic Society, 2019, 38(11): 3403-3408 (in Chinese).

[9] LIAN L, SOTTOS N R. Effects of thickness on the piezoelectric and dielectric properties of lead zirconate titanate thin films[J]. Journal of Applied Physics, 2000, 87(8): 3941-3949.

[10] SAMANTA S, SANKARANARAYANAN V, SETHUPATHI K. Effect of Nb and Fe co-doping on microstructure, dielectric response, ferroelectricity and energy storage density of PLZT[J]. Journal of Materials Science: Materials in Electronics, 2018, 29(23): 20383-20394.

[11] . PZT [D]. : , 2019.
ZHANG J. Flexible heterogeneous integration fabrication and study on electrical performance of PZT piezoelectric thin film[D]. Taiyuan: North University of China, 2019 (in Chinese).

[12] FUJII E, TAKAYAMA R, NOMURA K, et al. Preparation of (001)-oriented Pb(Zr, Ti)O_3/thin films and their piezoelectric applications[J]. IEEE Transactions on Ultrasonics, Ferroelectrics, and Frequency Control, 2007, 54(12): 2431.

[13] MIYAZAKI H, MIWA Y, SUZUKI H. Improvement in fatigue property for a PZT ferroelectric film device with SRO electrode film prepared by chemical solution deposition[J]. Materials Science and Engineering: B, 2007, 136(2/3): 203-206.

[14] DOI H, KAGEYAMA K. Effect of metallic oxides containing composite electrodes on crystallization and ferroelectric properties of Pb($Zr_{0.52}$, $Ti_{0.48}$)O_3 thin films deposited by the Sol-gel method[J]. Journal of Sol-Gel Science and Technology, 1999, 16(1): 21-27.

[15] CHIOU Y K, WU T B. Characteristic of (100)-textured (Pb_xSr_{1-x})TiO_3 thin films used for dram and tunable device application[J]. Integrated Ferroelectrics, 2006, 80(1): 395-405.

[16] WANG C, FANG Q F, ZHU Z G, et al. Dielectric properties of Pb($Zr_{20}Ti_{80}$)O_3/Pb($Zr_{80}Ti_{20}$)O_3 multilayered thin films prepared by rf magnetron sputtering[J]. Applied Physics Letters, 2003, 82(17): 2880-2882.

[17] JEONG Y S, LEE H U, LEE S G, et al. Annealing effect of platinum-based electrodes on physical properties of PZT thin films[J]. Current Applied Physics, 2009, 9(1): 115-119.

[18] VILQUIN B, LE RHUN G, BOUREGBA R, et al. Effect of in situ Pt bottom electrode deposition and of Pt top electrode preparation on PZT thin films properties[J]. Applied Surface Science, 2002, 195(1/2/3/4): 63-73.

[19] LI Q, WANG X, WANG F A, et al. Effect of neodymium substitution on crystalline orientation, microstructure and electric properties of Sol-gel derived PZT thin films[J]. Ceramics International, 2018, 44(7): 7709-7715.

[20] MA S, CHENG X W, ALI T, et al. Influence of tantalum on mechanical, ferroelectric and dielectric properties of Bi-excess $Bi_{3.25}La_{0.75}Ti_3O_{12}$ thin film[J]. Applied Surface Science, 2019, 463: 1141-1147.

[21] YANG J K, KIM W S, PARK H H. Enhanced fatigue property through the control of interfacial layer in Pt/PZT/Pt structure[J]. Japanese Journal of Applied Physics, 2000, 39(Part 1, No. 12B): 7000-7002.

[22] BOSE A, SREEMANY M. Influence of processing conditions on the structure, composition and ferroelectric properties of sputtered PZT thin films on Ti-substrates[J]. Applied Surface Science, 2014, 289: 551-559.

[23] RANJAN R, KUMAR R, BEHERA B, et al. Effect of Sm on structural, dielectric and conductivity properties of PZT ceramics[J]. Materials Chemistry and Physics, 2009, 115(1): 473-477.

[24] PARASHAR S K S, CHOUDHARY R N P, MURTY B S. Electrical propeties of Gd-doped PZT nanoceramic synthesized by high-energy ball milling[J]. Materials Science and Engineering: B, 2004, 110(1): 58-63.

[25] ARA JO E B, EIRAS J A. Effects of crystallization conditions on dielectric and ferroelectric properties of PZT thin films[J]. Journal of Physics D: Applied Physics, 2003, 36(16): 2010-2013.

[26] WEN B H, ZHANG Y, LIU X L, et al. Fatigue improvement in modified lead zirconate titanate ceramics through employment of $La_{0.8}Sr_{0.2}MnO_3$ buffer layers[J]. Ceramics International, 2013, 39(1): 219-225.

(下转第 760 页)

Journal of Materials Chemistry, 2010, 20(43): 9695.

[22] PARK D G, DUCHAMP J C, DUNCAN T M, et al. Preparation of forsterite by pyrolysis of a xerogel: the effect of water[J]. Chemistry of Materials, 1994, 6(11): 1990-1995.

[23] LI Z H, YU Q J, CHEN X W, et al. The role of MgO in the thermal behavior of MgO-silica fume pastes[J]. Journal of Thermal Analysis and Calorimetry, 2017, 127(3): 1897-1909.

[24] BERNARD E, LOTHENBACH B, RENTSCH D, et al. Formation of magnesium silicate hydrates (M-S-H)[J]. Physics and Chemistry of the Earth, Parts A/B/C, 2017, 99: 142-157.

[25] , , , . MgO $MgO-SiO_2-H_2O$ [J]. , 2019, 47(2): 220-227.
SONG Q, HU Y R, WANG Q, et al. Effect of MgO reactivity and curing temperature on properties of $MgO-SiO_2-H_2O$ system[J]. Journal of the Chinese Ceramic Society, 2019, 47(2): 220-227 (in Chinese).

[26] MILLER F A, WILKINS C H. Infrared spectra and characteristic frequencies of inorganic ions[J]. Analytical Chemistry, 1952, 24(8): 1253-1294.

[27] LIPPMAA E, MAEGI M, SAMOSON A, et al. Structural studies of silicates by solid-state high-resolution silicon-29 NMR[J]. Journal of the American Chemical Society, 1980, 102(15): 4889-4893.

[28] LIPPMAA E, MAEGI M, SAMOSON A, et al. Investigation of the structure of zeolites by solid-state high-resolution silicon-29 NMR spectroscopy[J]. Journal of the American Chemical Society, 1981, 103(17): 4992-4996.

[29] WEISS C A, ALTANER S P, KIRKPATRICK R J. High-resolution ^{29}Si NMR spectroscopy of 2 1 layer silicates: correlations among chemical shift, structural distortions, and chemical variations[J]. American Mineralogist, 1987, 72(9-10): 935-942.

[30] ROOSZ C, GRANGEON S, BLANC P, et al. Crystal structure of magnesium silicate hydrates (M-S-H): the relation with 2 1 Mg-Si phyllosilicates[J]. Cement and Concrete Research, 2015, 73: 228-237.

[31] NIED D, DAUZÈRES A. Magnesium silicate hydrates (M-S-H): formation kinetics and range of composition [J]. Magnesium, 2014, 14: 17.

[32] ENGELHARDT G, KOLLER H. 29Si NMR of inorganic solids[M]//Solid-State NMR II. Berlin, Heidelberg: Springer Berlin Heidelberg, 1994: 1-29.

(上接第 750 页)

[27] CHEN F, CHENG J R, YU S W, et al. Structural and electrical properties of $Pb(Zr_{0.53}Ti_{0.47})O_3$ films prepared on $La_{0.5}Sr_{0.5}CoO_3$ coated Si substrates[J]. Journal of the European Ceramic Society, 2010, 30(2): 453-457.

[28] KUMAR P, SINGH P, SINGH S, et al. Influence of lanthanum substitution on dielectric properties of modified lead zirconate titanates[J]. Ceramics International, 2015, 41(3): 5177-5181.

[29] SUI H T, SUN H J, LIU X F, et al. Ferroelectric and dielectric behaviors of Sol-gel derived perovskite PMN-PT/PZT heterostructures via compositional development: an interface-dependent study[J]. Journal of the European Ceramic Society, 2018, 38(16): 5382-5387.

[30] JIANG Q Y, CAO W W, CROSS L E. Electric fatigue in lead zirconate titanate ceramics[J]. Journal of the American Ceramic Society, 1994, 77(1): 211-215.